

## Analytical Design of a High-Torque Flux-Switching Permanent Magnet Machine by a Simplified Lumped Parameter Magnetic Circuit Model

Mr. Malloji Mallesham  
Asst Professor

Department of Mechanical Engineering Princeton College of Engineering Hyderabad

**Abstract** -- This paper presents how to analytically design a high-torque three-phase flux-switching permanent magnet machine with 12 stator poles and 14 rotor poles. Firstly, the machine design parameters are studied addressing on high output torque and its flux distribution is also investigated by finite-element method (FEM) analysis. Then a simplified lumped parameter magnetic circuit model is built up for analyzing design parameters. And a design procedure is also presented. The analytically designed machine is verified by FEM simulations.

### INTRODUCTION

FLUX-SWITCHING permanent magnet (FSPM) machines having PMs in the stator with doubly salient stator and rotor structure like a switched reluctance machine combine the advantage of a conventional PM machine and a switched reluctance machine. They have therefore high reliability, high torque /power density and relatively high efficiency, hence preferable for reliability premium applications. Today FSPM machines have been presented for different applications, such as in aerospace, automotive and wind energy applications [1]-[3]. Several papers have investigated different FSPM machines with various stator and rotor pole combinations and their characteristics [4]- [11]. In [4] and [9] a FSPM machine with 12 stator poles and 14 rotor poles (12/14 poles) as shown in Fig. 1 has been investigated. Compared with a 12/10 pole machine, this machine can provide higher torque density with less torque ripple

Today FSPM machines are generally designed as an initial machine, in which  $H_{sb} = I_{pm} = W_{rt} = W_s = W_{st} = \tau_s / 4$  as shown in Fig. 2, thereafter the optimal parameters and /or performance were studied by either finite element method (FEM) simulations or lumped parameter magnetic circuit model [8] [11][14]. Such

initially designed FSPM machines usually have highly saturated stator iron teeth that is normally beneficial for a 12/10 pole machine to improve the output torque. But for a 12/14 pole machine, the high saturation will lead to a torque decrease due to the high flux leakage between the stator and rotor [9]. So a new approach is required to design a high-torque 12/14 pole machine. This paper introduces a simplified lumped parameter magnetic circuit model to analytically design the machine. Firstly the machine design parameters are studied addressing on high output torque. Then the flux distribution of a typical 12/14 FSPM machine is investigated by FEM simulations, based on which a lumped parameter magnetic circuit model is built up for finding optimal design parameters. Finally, the analytically designed machine is verified by FEM simulations.

For the design of an in-wheel traction system, there are two possible topologies, namely, direct driving and indirect driving. In a direct-driving system, the electrical motor is directly driving the wheel without a gearbox, as shown in Figure 1(b). This direct-driving in-wheel module provides a maximum simplicity for the system design; thus, it

is commonly adopted in most existing in-wheel traction systems.

However, due to the absence of gearbox, the electrical motor of a direct-driving system needs to provide a high torque. The high torque in-wheel motor increases the wheel mass and consequently reduces the passenger comfort [3]. To solve this problem, an indirect-driving in-wheel module, shown in Figure 2(a), can be adopted, in which the electrical motor is indirectly driving the wheel through a gearbox. By this means, the required torque for the motor is reduced (Figure 2(b)), and the wheel mass is maintained. Different topologies of the in-wheel traction lead to different requirements and constraints for the motor design. Nevertheless, in both topologies, electrical motors need to have a high torque density with certain level of ruggedness.

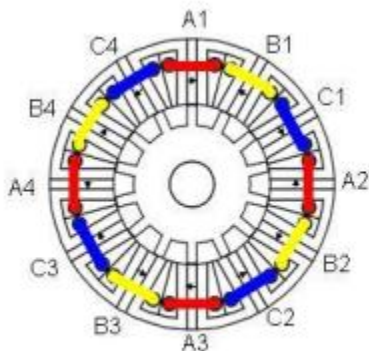


Fig. 1. Cross section of a 12/14 pole machine.

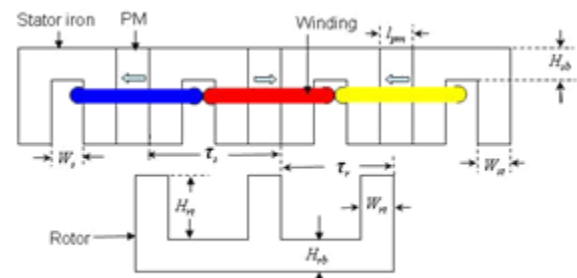


Fig. 2. Part of an initial machine in a plain form.

## MACHINE CONSTRUCTION

Fig. 1 shows the machine construction. Each phase winding of the machine consists of four coils and each coil is concentrated around two stator teeth with a magnet inset in between. The magnets are circumferentially magnetized and the magnetization is reversed in polarity from one magnet to the next. For each phase the flux in coils 1 and 2 are respectively the same as that in the corresponding phase coils 3 and 4 due to the symmetrical machine construction. The coil -flux linkage of each phase (the summary of four coils) is essentially sinusoidal with respect to the rotor position and has a period of  $\tau$  as shown in Fig. 3. And it reaches the peak value when the rotor is at the d-axis position of the phase as shown Fig. 4 (a). At this position the fluxes in the four coils of the phase are the same, as can be seen in Fig. 5 in which the fluxes in coils A1, A2, A3 and A4 are the same.

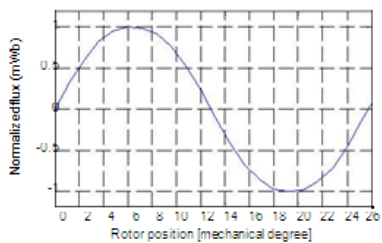


Fig. 3 Coil-flux linkage in one phase

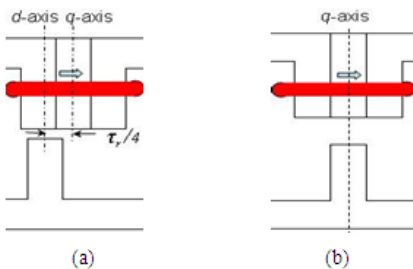


Fig. 4. Rotor at (a) *d*-axis position where the coil-flux linkage is maximum, (b) *q*-axis where the coil-flux linkage is zero.

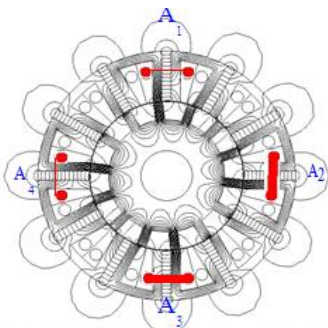


Fig. 5. Flux distribution at the *d*-axis position of phase  $\alpha$ .

MACHINE DESIGN

A. Design parameters

If neglecting machine losses the torque of a 12/14 pole FSPM machine can be expressed as [9]

$$T = \frac{2\pi^2 k P}{4P_s} B_t^2 D^2 L S_c \quad (1)$$

where  $B_t$  is the average flux density in the stator tooth at the *d*-axis position, and  $k_\sigma$  is the leakage factor

representing the effective flux for torque production at the *d*-axis position and evaluated here by

$$k_\sigma = \frac{\Phi_{p3} - \Phi_{p4}}{\Phi_{p3}} \quad (2)$$

where  $\Phi_{p3}$  and  $\Phi_{p4}$  are respective the flux through the teeth *P3* and *P4* in Fig. 8.

The parameters  $D_o$  and  $L$  are generally constrained by the available volume of a specific case and are therefore fixed. In this paper they are respectively 100 mm and 200 mm

$B_t$  is an important design parameter. Ideally without considering iron saturation, the higher  $B_t$ , the higher torque from (1) would be produced. In reality, along with an increase of  $B_t$  the value of  $k_\sigma$  will decrease because of the increased iron saturation. This has been proven by FEM analysis as presented in Fig. 6, in which  $B_t$  is varied by using different magnet materials with various  $B_r$  from 0.6 -1.2 T, whilst keeping the machine dimension parameters unchanged. Since the output torque depends on both  $B_t$  and  $k_\sigma$ , their product value that directly indicates the torque capability of the machine is also shown in the figure. It is observed that the product reaches its peak value when  $B_t$  is 1.8 ~1.9 T. With a further increased  $B_t$  the leakage flux  $\Phi_{p4}$  increases more than the total flux  $\Phi_{p3}$  due to the iron saturation as shown in Fig. 7. As consequence, the effective flux,  $\Phi_{p3} - \Phi_{p4}$ , for torque production decreases, hence the leakage factor  $k_\sigma$  determined by (2). In this paper  $B_t$  is chosen to be 1.8 T, which is typically the saturation flux density of iron materials.

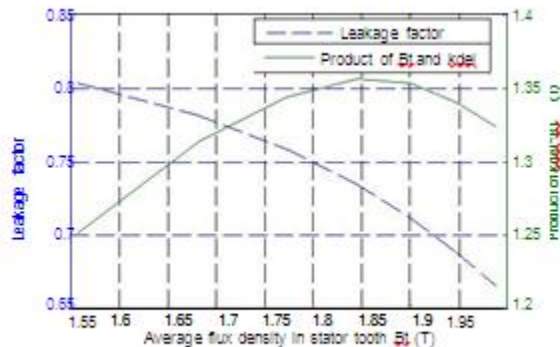


Fig. 6.  $k_{\sigma}$  and the product of  $B_t \cdot k_{\sigma}$  as function of  $B_t$  from FEM analysis.

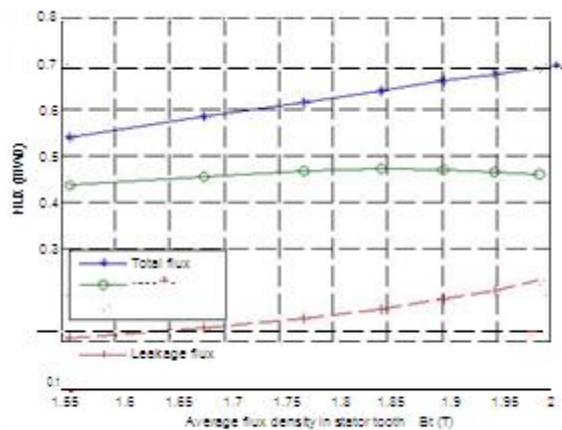


Fig. 7. The total, effective and leakage flux at different flux density

**Design procedure**

To calculate the maximum output torque from (1) with certain  $\lambda$  and  $c_s$ , the value of  $k_{\sigma}$  should be known when  $B_t$  is 1.8 T. This is achieved by gradually increasing  $l_{pm}$  based on the given initial value, then recalculating  $W_{rt}$  from (9) and further all the permeances in Fig. 9. Thereafter, solving the model to figure out  $\Phi_{p3}$  and  $\Phi_{p4}$  and further  $k_{\sigma}$  and  $B_t$ . Repeating the process until  $B_t = 1.8$  T. Now  $l_{pm}$  and  $k_{\sigma}$  are known and the output torque can be evaluated by (1).

Fig. 11 presents the design procedure

**Designed machine**

Fig. 12 shows the leakage factor as function of  $\lambda$  and  $c_s$ . For each  $c_s$  the value of  $k_{\sigma}$  increases along with an increase of  $\lambda$ , and for each  $\lambda$  there is an optimal  $c_s$  where  $k_{\sigma}$  reaches its maximum

value presents the output torque as function of  $\lambda$  and  $c_s$ . There is an optimal  $\lambda$  and  $c_s$  giving the maximum output torque. Fig. 14 and Fig. 15 respectively show the maximum output torque with respect to split ratio  $\lambda$  and stator tooth factor  $c_s$ . It is found that the optimal  $\lambda$  is around 0.5 and  $c_s$  is around 0.25 for the discussed case here. Table I lists the parameters of the designed machine

It should be noted that the magnet demagnetization and the maximum allowable temperature of the winding insulation should be considered when selecting the current density. This is out of the scope and therefore is not discussed in this paper.

**FEM SIMULATION**

To verify the result, the machine with the parameters given in Table I is investigated by 2D-FEM simulations, in which the  $B-H$  curve in Fig. 10 is employed for the iron material and  $B_t$  determined by (12) is set to 1.09 T to take the temperature influence into account. Fig. 16 shows the flux distribution of the machine at the  $d$ -axis position with no load ( $J = 0$ ), from which  $B_t$  and  $k_{\sigma}$  are obtained. Fig. 17 presents the output torque from the simulation. And Table II lists the results from both the lumped parameter magnetic circuit model and the FEM simulations. The torque calculated from the circuit model is about 3.3% higher than that from the FEM simulations. They match each other satisfactorily.

**CONCLUSION**

This paper has introduced a simplified lumped parameter magnetic circuit model for analytically designing a high-torque 12/14 pole FSPM machine. And the design procedure of how to find out the optimal design parameters is also presented. The design machine has been verified by FEM simulations

**REFERENCES**

[1] Arwyn S. Thomas, Z. Q. Zhu, Richard L. Owen, Geraint W. Jewell and David Howe, "Multiphase Flux-Switching Permanent-Magnet Brushless Machine for Aerospace Application", *IEEE Trans. Ind. Appl.*, vol. 45, No. 6, pp. 1971-1981, November/December 2009.

[2] Fang, Z. X., Wang, Y., Shen, J. X., Huang, Z. W., "Design and analysis of a novel flux-switching



permanent magnet integrated-starter-generator” , PEMD 2008

- [3] Jiangzhong Zhang, Ming Cheng and Zhe Chen, “Optimal design of stator interior permanent magnet machine with minimized cogging torque for wind power application”, *Energy Conversion and Management* 49, 2008, pp. 2100-2105.
- [4] J. T. Chen, Z. Q. Zhu, A. S. Thomas and D. Howe, “Optimal combination of stator and rotor pole numbers in flux-switching PM brushless AC machines”, the proceeding of *ICEMS, 2008*, vol. 44, pp. 4659 – 4667.
- [5] W. Z. Fei and J. X. Shen, “Comparative study and optimal design of PM switching flux motors”. *UPEC’06*, 6-8 Sept. 2006, vol. 2 pp. 695- 699.
- [6] Yu Chen, Z. Q. Zhu and David Howe, “Three-Dimensional Lumped- Parameter Magnetic Circuit Analysis of Single-Phase Flux-Switching Permanent-Magnet Motor”, *IEEE Trans. Ind. Appl.*, vol. 44, No. 6, pp. 1701-1710, November/December 2008.
- [7] Richard L. Owen, Z.Q. Zhu, Arwyn S. Thomas, Geraint W. Jewell and David Howe, “ Alternate Poles Wound Flux-Switching Permanent- magnet Brushless AC Machines”, *IEEE Trans. Ind. Appl.*, vol. 46, No, 2, pp. 790-797, March/April, 2010.
- [8] Z. Q. Zhu, Y. Pang, D. Howe, S. Iwasaki, R. Deodhar, and A. Pride, “Analysis of electromagnetic performance of flux-switching permanent magnet machines by non-linear adaptive lumped parameter magnetic circuit model,” *IEEE Trans. Magn*, vol.41, No.11, pp. 4277- 4287, November 2005.
- [9] Anyuan Chen, Njål Rotevatn, Robert Nilssen and Arne Nysveen, “Characteristic Investigations of a New Three-Phase Flux-Switching Permanent Magnet Machine by FEM Simulations and Experimental Verification” in the proceeding of *ICEMS2009*, 15-18, Nov., 2009 Tokyo, Japan.
- [10] Emmanuel Hoang, Michel Lecrivain, Mohamed Gabsi, “A new structure of a switching flux synchronous poly-phased machine with hybrid excitation”, the proceeding of *Power electronics and applications*, 2007 European conference, pp. 1-8.
- [11] Z.Q. Zhu, Y. Pang, J. T. Chen, Z. P. Xia, D. Howe, “Influence of design parameters on output torque of flux-switch permanent magnet machines”, *IEEE VPPC*, 2008, September 3-5, 2008, Harbin, China.
- [12] P. Thelin and H-P Nee, “Calculation of the Airgap Flux Density of PM Synchronous Motors with Buried Magnets Including Axial Leakage and Teeth Saturation”, *EMD’99*, Canterbury, United Kingdom, September 1999, pp.339-345.
- [13] Wei Hua, Ming Cheng, Z. Q. Zhu and David Howe, “Analysis and optimization of back EMF waveform of a flux-switching permanent magnet motor”, *IEEE Transactions on Energy Conversion*, VOL. 23, NO. 3, September 2008, pp 727-733.